Constant Glucose Biosensor Based on Vertically Aligned Carbon Nanotube Composites

Amin TermehYousefi[1,], Samira Bagheri[2], Nahrizul Adib Kadri[3], Mohamad Rusop Mahmood[4], Shoichiro Ikeda[1]*

[1] ChECA IKohza , Dept. Environmental & Green Technology (EGT) , Malaysia Japan International Institute of Technology (MJIIT), University Technology Malaysia (UTM), Kuala Lumpur, Malaysia
[2] Nanotechnology & Catalysis Research Centre (NANOCAT), IPS Building, University Malaya, 50603 Kuala Lumpur, Malaysia
[3] Department of Biomedical Engineering, Faculty of Engineering, University Malaya, 50603 Kuala Lumpur, Malaysia
[4] NANO-SciTech Centre, Institute of Science, Universiti Teknologi MARA (UiTM), Shah Alam, Selangor, Malaysia
[*]E-mail: at.tyousefi@gmail.com

In this contribution, a reagent free glucose biosensor was prepared based on multi walled carbon nanotubes (MWCNTs) composite via the electrochemical method. The synthesized MWCNTs were in turn successfully optimized by the chemical vapor deposition (CVD) method. The glucose oxidase (GOx) was immobilized on a carbon nanotubes/gelatin (Gl) composite using the entrapment technique, with an 8.42 s^{-1} direct electron transfer rate between GOx and MWCNTs/Gl, which was then dropcasted onto a glassy carbon electrode (GCE). The bioactivity of GOx on modified GCE was retained during the electrochemical reactions. The cyclic voltammetric results coupled with the chronoamperometric response and obtained from modified GCE indicated that a GOx/MWCNTs/Gl/GC electrode can be utilized as a glucose biosensor via its display of high sensitivity and stability. The biosensor exhibited a wide linearity range to 8.9 mM glucose, with the detection limit of 0.54 mM and a stability of 75.4% current diminish after 25 days. The proposed fabrication method of glucose biosensor was in line with the developments of electrochemical research for glucose determination of human serum in the context of electrochemical reactions. The results indicated that the biosensor possessed good stability and acceptable fabrication reproducibility.

1. INTRODUCTION

Glucose measuring is a routine medical analysis procedure. A total of 5% of the population of developed countries are suffering from diabetes [1]. Thus, the development of new methods for simple, rapid, reliable, sensitive, reproducible glucose detection became rather imperative to researchers around the globe. The reliability of electrochemical techniques and precise biological recognition process prompted researchers to fabricate electrochemical biosensors in the simplest and most reliable scheme for the purpose of bio-sensing glucose [2]. To achieve enzyme-catalyzed oxidation of glucose at anodic potentials, the amperometric glucose biosensors with optimized features, such as selectivity and sensitivity, with fast response, small sizes, and good stability with lower costs is required [3]. Carbon nanostructures have been vastly used for this aim, due to its desirable properties. Carbon nanotubes (CNTs) particularly, display unrivaled properties in electrochemical biosensors, due to its high surface area for sensing interaction, as well as excessive sensitivity to chemical doping effects during the interplay with diverse biological molecules [4]. CNTs-based paste electrodes [5], electrodes modified by CNTs [6], metallic nanoparticles modified CNTs-based electrodes [7], and CNTs-based electrodes with immobilized enzymes [8] are some of the recent techniques being implemented for CNTs-based biosensors [9].

In order to optimize the reactivity of CNTs, they were modified to reclaim the oxidation or reduction of biological molecules during the adsorbent and interaction of biosensors. The total charge carrier of CNTs density will change by adsorbent biomolecules and the alteration of the conductance, making CNTs-based biosensor capable of powering a full device in continuous monitoring of biological molecules [10]. According to previous results, functionalization via enzymes is the most effective approach in modifying the surface of CNTs to make electrochemical biosensors [11, 12]. Polymeric entrapment or covalent immobilization methods enhances the direct and fast electron transfer of enzymes, and are rapidly emerging as a new research area in the functionalization of CNTs [13].

Gelatin is a natural polymer product obtained from collagen [14]. It is one of the major proteins in skin, bones, and white connective tissues, which are widely used in immobilization matrices for the preparation of biosensors [15]. Its great gel forming ability, as well as high biocompatibility with extremely heterogeneous polymer networks and different sizes of polypeptides and its molecular weight distribution in the range of 15,000 to 250,000 makes it ideal for the preparation of electrochemical biosensors [16]. Taking into account previous reports on the advantageous properties of gelatin in electrochemical biosensors [17, 18], the MWCNT gelatin matrix was used to improve the direct electron transfer processes between GOx and modified GCE through hydrophobic–hydrophobic interactions in forming stable dispersions of MWCNTs. The employed MWCNT were successfully synthesized on a silicon substrate in an optimized process, using renewable natural camphor oil via the chemical vapor deposition (CVD) method. A high linear range and advisable sensitivity for glucose was obtained with the GOx/MWCNTs/Gl/GC electrode. Additionally, high activity and excellent stability of fabricated glucose biosensor can offer desirable outcomes for glucose detection approaches based on functionalized MWCNT composites.

2. EXPERIMENTAL PROCEDURE

2.1 Chemicals and Apparatus

Glucose oxidase (GOx), Gelatin (from bovine bones), and D-Glucose and K3[Fe(CN)6] were purchased from Sigma–Aldrich Co., Ltd. (Malaysia). A phosphate buffer saline (PBS, pH 7) was utilized as its supporting electrolyte. Uric acid, ascorbic acid, cysteine, oxalic acid lactose, and sucrose were of analytical grade and purchased from Merck. Other reagents were purchased from Aldrich, and used as received without further purification.

All voltammetric analysis (cyclic voltammetry) were carried out with the Potentiostat/Galvanostat (Autolab, Metrohm (Netherlands)) coupled to a Pentium IV personal computer. The experiments were conducted using a conventional three-electrode electrochemical cell at room temperature. A modified glassy carbon electrode was used as a working electrode, while a saturated Ag|AgCl|KCl 3 M was used as a reference electrode, and a platinum wire was utilized as a counter electrode. All potentials were measured and reported against the Ag|AgCl|KCl 3M reference electrode. The CNTs was prepared by the chemical vapor deposition method and used to modify the working electrode.

The synthesized CNTs were characterized by FESEM (ZEISS Supra 40VP) operated at 5 kV to evaluate the structure and the aspect ratio of the sample. The Raman spectra were obtained using micro-Raman spectroscopy (Horiba Jobin Yvon-DU420A-OE-325) with Ar^+ ion (wavelength 514.5 nm) to determine the adsorption, desorption, and surface area of the samples. Hitachi H-9500 Transmission Electron Microscopy (TEM) and Hitachi S-3500N scanning electron microscope (SEM), equipped with electron diffraction analysis, was used for the chemical characterization of the specimens, as well as surface imaging. All experiments were conducted at room temperature.

2.2. Synthesis and Purification of MWCNTs

The experimental setup of growing MWCNTs is based on horizontal electronic furnaces covering the quartz tube during CNTs fabrication. Camphor oil, as a precursor, was mixed with ferrocene and introduced to the inlet of the quartz tube fitted by the first furnace to release the vaporized CNTs. The reaction temperature was increased to 180 °C, and maintained for 30 min to ensure that the precursor and catalysts were completely pyrolyzed. Ferrocene decomposes to form the iron catalyst necessary for the experiment, while camphor acts as a carbon source (feedstock) of the substrate in the second furnace. The CVD experiments began when the deposition temperature of the second furnace were optimal (825 °C). The exhaust argon gas in the quartz tube induced the movement of the amorphous vaporized carbon into the second furnace via a mass flow controller, thereby allowing CNT growth on the surface of the proposed substrate. After 1 h of reaction, a conventional cooling method was employed to slowly cool the reactor to room temperature in an Ar environment [19]. The MWCNTs were purified based on the literature by heating in the air at 600 °C for 100 min, and soaked in 6 M of hydrochloric acid (HCl) solution for 1 day, followed by centrifuging [20]. The

precipitate obtained by centrifuging was washed with deionized water (DI) and well dried under air. The MWCNTs were chemically functionalized by MWCNTs, according to the literature. MWCNTs were then briefly heated in air at 600 °C for 2 h, and then soaked in 6 M HCl solution for 24 h and centrifuged. The precipitate was rinsed with deionized water and dried under air. A mixture of sulfuric acid and nitric acid (3:1) was used to chemically functionalize MWCNTs via ultrasonic agitation for 8 h [21]. The functionalized MWNTs were then rinsed with DI water (until pH 7.0 was reached) and well dried after the separation process thrice by centrifuging the MWCNTs.

2.3. Fabrication of GOx /MWCNTs/Gl/GCE

We prepared the MWCNTs/gelatin composites by dispersing 1 mg of synthesized MWCNTs in 1 ml of 3% gelatin solution by 25 min ultra-sonication, and subsequently, the GOx was added to the MWCNTs/gelatin composite at a 1:1 volume ratio. The bare glassy carbon electrode was polished on chamois leather with 0.02 μm alumina powder, and sonicated in deionized water and absolute ethanol, respectively. Then 3μl of MWCNTs/gelatin/ GOx was drop casted onto a 3mm glassy carbon electrode, while the modified GC electrode was well dried at 4℃ for 12h.

3. RESULTS AND DISCUSSION
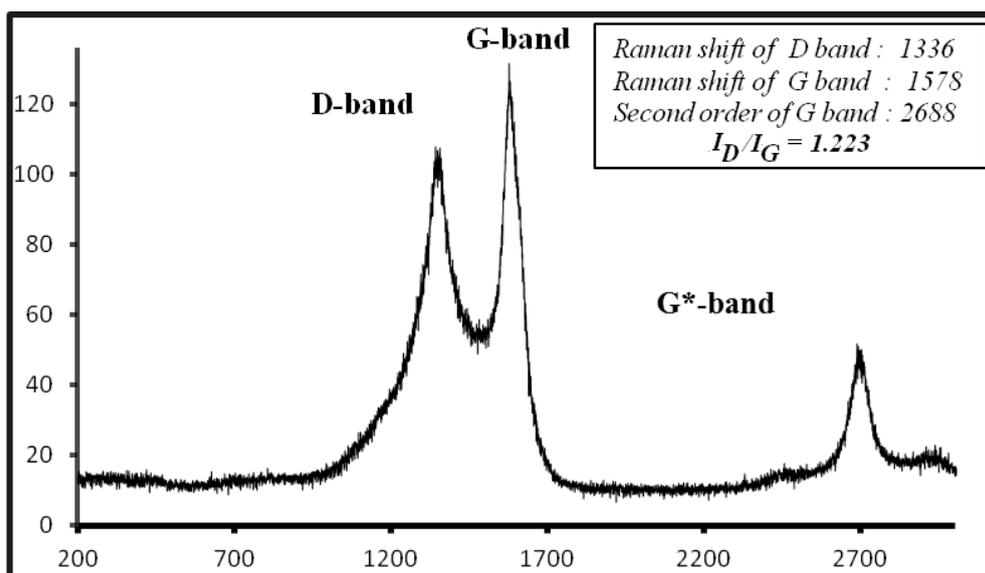
3.1. Raman Characterization

Figure 1. Raman spectra of synthesized MWCNTs. Inset is the Raman shifts of D-band and G-band to estimate the I_G/I_D

Figure 1 shows the Raman spectra of MWCNTs. Generally, peak intensities, ranging from approximately 1300 cm^{-1} to 1350 cm^{-1}, and approximately 1580 cm^{-1} to 1600 cm^{-1}, represent the

disordered D line and graphitic G line, respectively. The D peaks corresponding to the disorder of the multilayer vertical CNTs was 1346.35 cm^{-1}, while the G peak(s) was at ~1588.40 cm^{-1}. The I_G/I_D ratio, which was calculated to estimate the variation in the growth CNTs' quality, was 1.22. The absence of the radial breathing mode (RBM) in the Raman shift proves that the grown CNTs is more than likely to contain more than a single wall, or that the diameter of the growth CNTs exceeds 3 nm [22-24].

3.2. Electron Microscopy (EM) Characterization

3.2.1. Field Emission Scanning Electron Microscopy (FESEM)

As shown in Figure 2, the FESEM results corresponding to the growth mechanism of MWCNTs highlighted the high aspect ratio and uniformity of the synthesized CNTs using the CVD method. The average diameter of CNTs is enhanced by applying it at higher deposition temperatures, which leads to the growth of more crystalline CNTs with lower than average diameter. Using the data collected from the aspect ratio of the FESEM images, the growth rate of the nanotubes can be calculated using the formula $\alpha = \beta$ (µm) / γ (min), where β is the distribution length of the tubes, and γ is the deposition time. Therefore, the growth rate of the synthesized CNTs is 3.03 µm/min at 30 minutes deposition time, which included the optimized temperature and time [25].
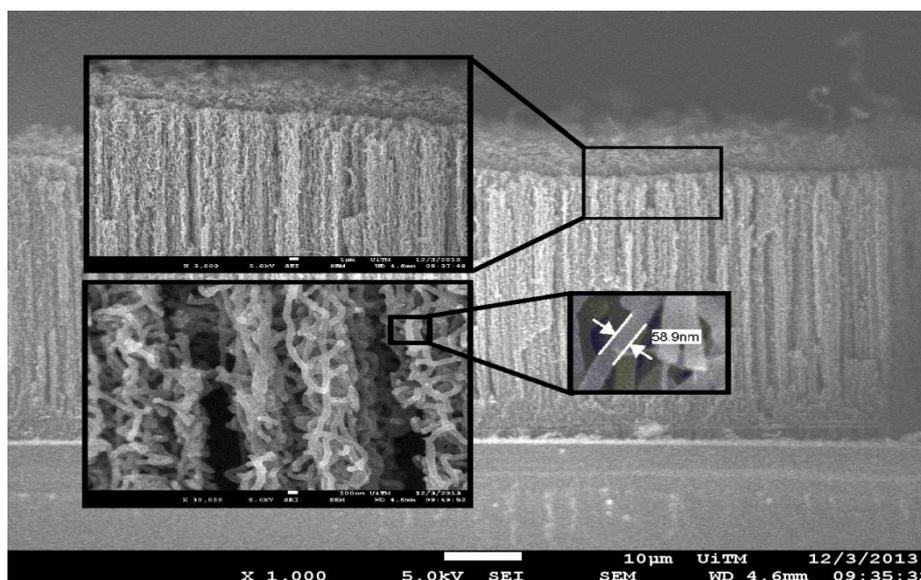

Figure 2. SEM image of synthesized MWCNTs

3.2.2. Transmission Electron Microscopy (TEM)

Figure 3 shows the TEM results of the grown MWCNTs via the CVD method. Most of the tubes are closed, and the feedstock is well graphitized. The TEM image also confirms the complete removal of catalyst particle and the absence of amorphous carbon. The results also indicated that each CNT wall is made up of 10-15 graphitic sheets [26].
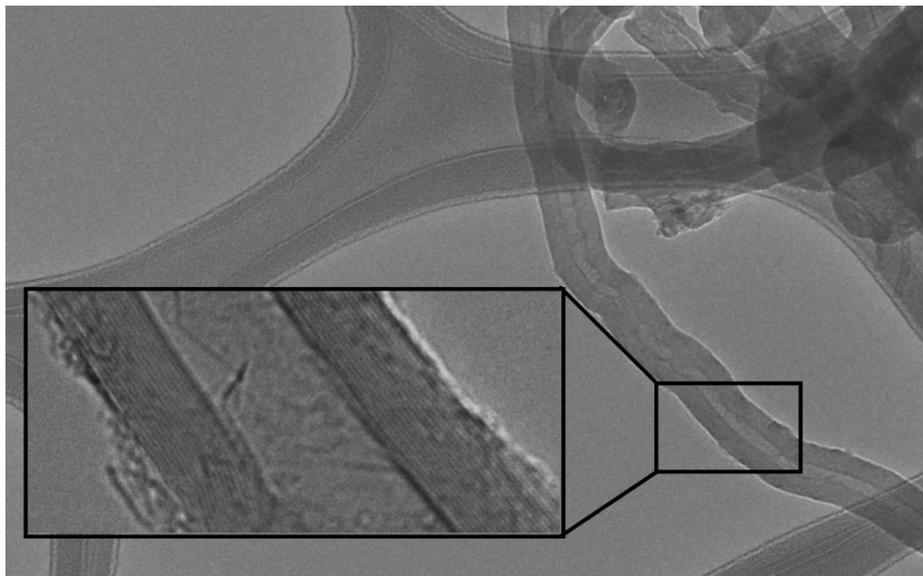
Figure 3. TEM image of synthesized MWCNTs

3.3 Direct electron transfer of GOx /MWCNTs/Gl/GCE

The cyclic voltammograms of GOx/MWCNTs/Gl/GCE in nitrogen saturated pH 7 PBS at different scan rates in the range of 20-200 mV/s is shown in Figure 4a. The well-defined and nearly symmetric redox peaks are detected with a formal potential of +0.3 V.
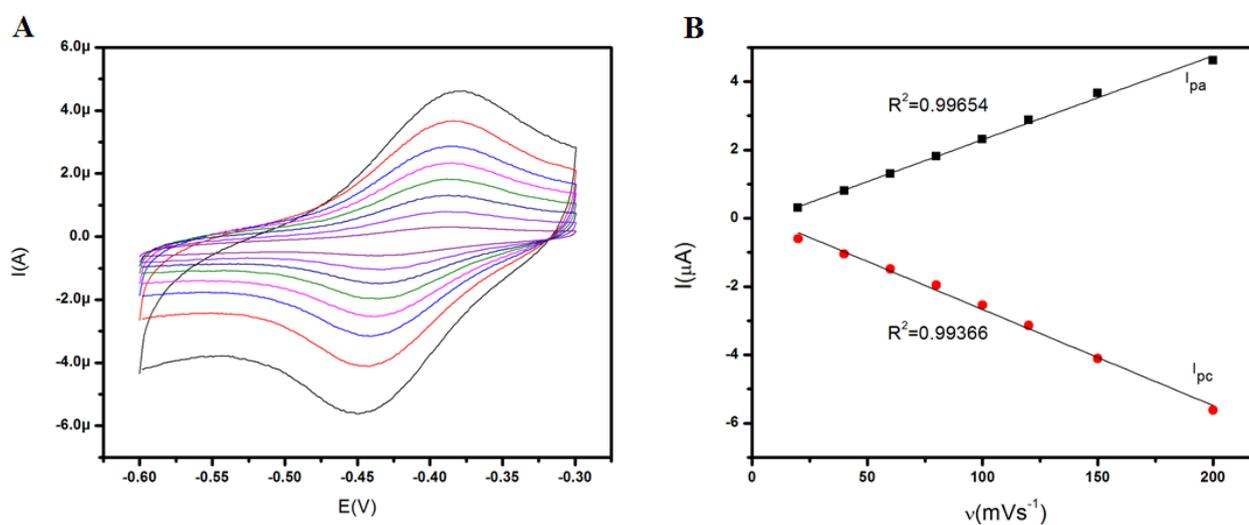

Figure 4. A) Cyclic voltammograms of the GOx/MWCNTs/Gl/GCE in 0.1 M PBS with nitrogen saturated at different scan rates (from inner to outer curves: 20, 40, 60, 80, 100, 120, 150, 200 mV/s). B) Ipa and Ipc vs. scan rates.

The controlled electrodes illustrated that the redox peaks are derived from GOx, which is similar to the reported results [27, 28]. The peak separation (ΔEp), ranging from 25 mV at a scan rate

of 20 mV s^{-1}, to 65 mV at 200 mV s^{-1}. The redox peaks showed that GOx entrapped in the nanocomposite film undergoes a quasi-reversible electron transfer process [29]. According to the cyclic voltammograms of the GOx/MWCNTs/Gl/GCE, the electron transfer between the electrode and the active site of GOx was not shielded by the globular protein shell of GOx. Figure 4.b shows a linearity of the anodic or cathodic peak currents at different scan rates, which confirms the surface-confined electrode reactions. The electron transfer rate between the electrode and GOx was determined to be 8.42 s^{-1} using the Laviron's method [30]. Meanwhile, it was also observed that the matrix prominently facilitates active sites of GOx in its approach to the electrode, and confirmed that the GOx/MWCNTs/Gl is stable on glassy carbon electrode [31].

3.4. Biocatalytic Activity of GOx/MWCNTs/Gl/GC Electrode

Figure 5 demonstrates the cyclic voltammograms of the GOx/MWCNTs/Gl/GCE in nitrogen saturated pH 7 PBS containing 0.5 mM potassium ferricyanide as its mediator. Figure 5.a describes the redox behavior of potassium ferricyanide on GOx/MWCNTs/Gl/GCE in the absence of glucose, while Figure 5.b ascribes the redox behaviors when 1.3 mM glucose was added into the solution. It was observed that the redox anodic peak current increases. These behaviors demonstrated that GOx/MWCNTs/Gl/GCE is capable of electrocatalyzing the glucose oxidation by taking potassium ferricyanide as a mediator in nitrogen saturated solutions [32, 33].

To optimize the sensitivity and stability of the biosensor by chronoamperometric measurement, the amount of enzyme loading and pH of the buffer were studied. The mix pH 7 PBS, containing 1 mg of GOx with 1 ml of MWCNTs/Gl composite, shows a maximum response of 1.3 mM glucose at an applied potential of +0.3 V. Consequently, this optimized volume ratio of GOx solution and nanocomposite was used to prepare the biosensor. The dependence of pH from 6.0 to 8.0 on the response, to 1.3 mM glucose in the presence of potassium ferricyanide (0.5 mM) for the biosensor was explored at an applied potential of +0.3 V, allowing us to obtain the highest current response that correspond to a pH of 7 [34].
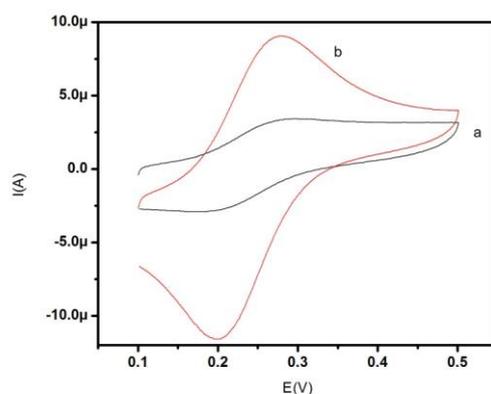

Figure 5. a) Cyclic voltammograms of the GOx/MWCNTs/Gl/GCE at scan rate of 20 mV/s in 0.1 M nitrogen saturated PBS and 0.5 mM potassium ferricyanide, a) in absence of glucose, b) in the presence of 1.3 mM glucose.

3.5. Amprometric determination of glucose on GOx/MWCNTs/Gl/GC Electrode

The characteristics of the GOx/MWCNTs/Gl/GC electrode at optimal conditions obtained previously were investigated by chronoamperometric measurement. Figure 6.a displays a representative current–time response for the successive addition of 1.3mM of glucose in each successive adding. The calibration curve in Figure 6.b, with a dynamic linear range, spans the glucose concentration from 0.1 to 8.9 mM, and at higher concentrations, it deviates from linearity, which represents a typical Michaelis–Menten kinetics characteristic. The sensitivity of fabricated modified glassy carbon electrode is 0.244 μAmM^{-1}, which is higher than the reported 0.183μAmM^{-1} [35].

According to the results, the fabricated biosensor has higher biological affinity to glucose. The immobilized process might result in the micro-environment changing the enzyme and affecting its intrinsic properties, which could improve its affinity to glucose. The direct electron transfer of GOx in the biosensor exhibits higher stability, and its voltammetric response remains stable after a continuous potential scanning for 75 cycles. After the electrochemical measurement, the sensor was rinsed with deionized water and stored, and accordingly, there is nearly no decrease of the catalytic current to glucose after keeping the biosensor for 25 days at 4 °C. Some possible interference species, such as ascorbic acid, cysteine, uric acid, lactose and sucrose on the detection of glucose were subsequently investigated.
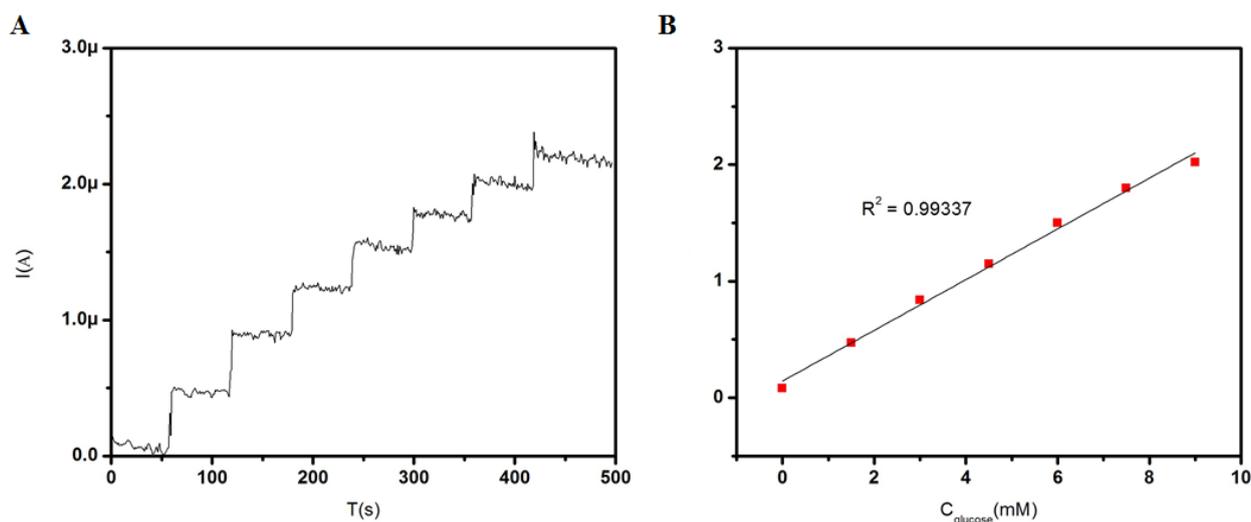

Figure 6. A) The chronoamperometric response of GOx/MWCNTs/Gl/GCE on successive addition of 1.3 mM glucose in each successive adding at applied potential of +.3 V. **B)** The calibration curve of the electrocatalytic current on different concentration of glucose.

3.6. Reproducibility and stability of GOx/MWCNTs/Gl/GC Electrode

The storage stability and reproducibility of the modified GOx/MWCNTs/Gl/GC electrode were also studied. The relative standard deviation (RSD) of the modified electrode response to 1.3 mM glucose was 2.6–5.6 % for five successive additions. The RSD for detection of 1.3 mM glucose with four modified electrodes prepared under the same conditions was 3.4–6.1 %. When the modified

electrode was stored dry and measured at intervals of 1 week, it retained about 75.4% of its original sensitivity after 25 days.

3.7. Determination of glucose in human blood serum and analytical recovery of glucose

The response of the modified electrode to the glucose in human serum of blood was examined. The blood serum sample attained from hospitalized patient was studied. The results were coordinated with referenced value gained by the standard colorimetric method in the hospital. Table 1 displays analytical recovery of the glucose solution, which was added to the PBS solution, suggesting the good accuracy of the modified electrode.

Table 1. Assay of glucose in human blood serum sample and recovery of glucose in PBS solution

Sample	Added (mM)	Biochemical analyzer in hospital (mM)	Found Mean Recovery (mM)	Recovery (%)
Serum of blood	-	4.60	4.47	-
Glucose	0.15	-	0.14	93±2

4. CONCLUSIONS

The entrapment of GOx in MWCNTs/Gl composite matrix was carried out with good film-forming and optimum bio-compatibility. The direct electron transfer of GOx reached a rate of 8.42 s^{-1} due to the approach of GOx's active sites to the modified electrode. The GOx/MWCNTs/Gl/GCE was superior in maintaining the bioactivity of GOx, rendering it is suitable as an amperometric biosensor for glucose detection with potassium ferricyanide as its mediator. The biosensor exhibited a wide linearity range of 0.1 mM to 8.9 mM glucose, with the detection limit of 0.54 mM and a stability of 75.4% current diminish after 25 days.

References

1. D. Meetoo, P. McGovern, and R. Safadi, *Am J. Nurs*, 16(2007),1002-1007.
2. N. J. Ronkainen, H. B. Halsall, and W. R. Heineman, *J.ChemSocRev*, 39(2010),1747-1763.
3. A. L. Ghindilis, P. Atanasov, and E. Wilkins, *J.Electroanalysis*, 9(1997),661-674.
4. C. Cai and J. Chen, *J. Anal. Biochem*, 332(2004),75-83.
5. Y. Lin, W. Yantasee, and J. Wang, *J. Front. Biosci*, 10(2005),582.
6. S. Wang, Q. Zhang, R. Wang, S. Yoon, J. Ahn, D. Yang, J. Tian, J. Li, *J. Electrochem. Commun.*, 5(2003),800-803.
7. H. Tang, J. Chen, S. Yao, L. Nie, G. Deng, and Y. Kuang, *J. Anal. Biochem.*, 331(2004),89-97.
8. Y. Lin, F. Lu, Y. Tu, and Z. Ren, *J. Nano Lett.*, 4(2004),191-195.
9. A. TermehYousefi, s. Bagheri, N. Adib, *J. Sensor rev*, 35(2015).
10. S. Hanna Varghese, R. Nair, B. G Nair, T. Hanajiri, T. Maekawa, Y. Yoshida, and D. Sakthi Kumar, *J.Curr Nanosci*, 6(2010),331-346.

11. W. Yang, P. Thordarson, J. J. Gooding, S. P. Ringer, and F. Braet, *J. Nanotechnology*, 18(2007),412001.
12. J. Wang and Y. Lin, *J. Trends Anal. Chem*, 27(2008),619-626.
13. T. Ahuja, I. A. Mir, and D. Kumar, *J. Biomaterials*, 28(2007),791-805.
14. V. Crescenzi, A. Francescangeli, and A. Taglienti, *J. Biomacromolecules*, 3(2002),1384-1391.
15. D. B. Khadka and D. T. Haynie, *J. Nanomedicine*, 8(2012),1242-1262.
16. A. Guiseppi-Elie, *J. Biomaterials*, 31(2010),2701-2716.
17. C. Ozdemir, F. Yeni, D. Odaci, and S. Timur, *J. Food Chem.*, 119(2010),380-385.
18. A. K. Sarma, P. Vatsyayan, P. Goswami, and S. D. Minteer, *J. Biosensors and Bioelectronics*, 24(2009),2313-2322.
19. A. TermehYousefi, S. Bagheri, K. Shinji, J. Rouhi, M. Rusop Mahmood, and S. Ikeda, *J. Biomed Res Int*, (2014).
20. S. K. Pillai, S. S. Ray, and M. Moodley, *J. JNN*, 7(2007),3011-3047.
21. X. Xing, S. Liu, J. Yu, W. Lian, and J. Huang, *J. Biosensors and Bioelectronics*, 31(2012),277-283.
22. J. Yun, C. Lee, Q. Zheng, and S. Baik, *J. JNN*, 12(2012),6534-6537.
23. A. Termehyousefi, S. Bagheri, N. Kadri, F. M. Elfghi, M. Rusop, and S. Ikeda, *J. Mater. Manuf. Processes*, 30(2015),59-62.
24. S. Sung, S. Tsai, C. Tseng, F. Chiang, X. Liu, and H. Shih, *J. Appl. Phys. Lett.*, 74(1999),197-199.
25. A. Termeh Yousefi, S. Bagheri, K. Shinji, M. Rusop Mahmood, and S. Ikeda, *J. Mater. Res. Innovations*, (2014).
26. M. Kumar and Y. Ando, *J. JNN*, 10(2010),3739-3758.
27. Y. Yin, Y. Lü, P. Wu, and C. Cai, *J. Sensors*, 5(2005),220-234.
28. X. Tu, Y. Zhao, S. Luo, X. Luo, and L. Feng, *J. Microchim. Acta*, 177(2012),159-166.
29. A. Guiseppi-Elie, C. Lei, and R. H. Baughman, *J. Nanotechnology*, 13(2002),559.
30. E. Laviron, *J. Electroanal chem*, 101(1979),19-28.
31. M. Pellissier, F. Barrière, A. J. Downard, and D. Leech, *J. Electrochem Commun*, 10(2008),835-838.
32. Y. Liu, M. Wang, F. Zhao, Z. Xu, and S. Dong, *J. Biosens Bioelectron*, 21(2005),984-988.
33. F. Chekin, S. Bagheri, A. K. Arof, and S. B. A. Hamid, *J. Solid State Electr*, 16(2012),3245-3251.
34. D. Zhang, K. Zhang, Y. L. Yao, X. H. Xia, and H. Y. Chen, *J. Langmuir*, 20(2004),7303-7307.
35. G. Cui, S. J. Kim, S. H. Choi, H. Nam, G. S. Cha, and K.-J. Paeng, *J. Anal Chem*, 72(2000),1925-1929.